

Magnetic coupling between folded cantilevers for high-efficiency broadband energy harvesting

Xuan Wu, Dong-Weon Lee*

MEMS and Nanotechnology Laboratory, School of Mechanical Engineering, Chonnam National University, Gwangju 500757, South Korea



ARTICLE INFO

Article history:

Received 18 May 2015

Received in revised form 25 July 2015

Accepted 15 August 2015

Available online 24 August 2015

Keywords:

Energy harvesting

Non-contact magnetic coupling

Frequency detuning

Multi-cantilevers

Broad bandwidth

ABSTRACT

In this paper, we proposed and characterized a high-efficiency piezoelectric energy harvester based on a non-contact coupling technique. The proposed design takes advantage of a frequency detuning technique and multi-cantilevers to enhance its power generation efficiency at ambient excitation. The energy harvester consists of two folded piezoelectric cantilevers with different resonance frequencies. A piezoelectric cantilever with a low resonance frequency (L-part) is coupled with another piezoelectric cantilever with a high resonance frequency (H-part) by a non-contact magnetic force. The output characteristic of each piezoelectric cantilever is improved using the magnetic coupling technique and a broad bandwidth is also realized under environmental vibrations. A feasibility of the fabricated energy harvester is experimentally confirmed to demonstrate the power generation capability in practical applications. With a load resistance of 50 kΩ, a maximum output power of 20 μW and an average power of 7.1 μW are achieved with the energy harvester, thus making it a suitable power supply for sensor nodes in wireless sensor network applications.

© 2015 Elsevier B.V. All rights reserved.

1. Introduction

As the demand for real-time information communication increases, wireless sensor network (WSN) technology plays a key role in various fields, owing to its advanced continuous detection and information monitoring capability [1–3]. However, because batteries employed in commercial WSNs have a limited life, the frequent replacement of batteries results in significant maintenance costs and considerable inconvenience. To overcome this limitation, various energy harvesters that can scavenge unlimited ambient energy to power the sensor nodes in WSNs have been developed as substitutes for batteries [4–6].

Vibration energy exists pervasively in our living environment and is therefore considered as the main power source for energy harvesting. Although several mechanisms have been designed for harvesting vibrational energy, piezoelectric energy harvesting has become one of the most effective methods to scavenge energy from environmental vibrations owing to its power efficiency and favorable miniaturization ability [7–10]. However, ambient vibration often spans a broad low-frequency range, i.e., 0–40 Hz [11]. Because of the frequency mismatch between the high resonant frequency (~hundreds or thousands of Hertz) of many vibration energy harvesters and the ambient low-frequency vibrations, power

is generated inefficiently [12]. To overcome the frequency gap between the environmental vibration and energy harvesters, various designs based on the frequency up-conversion concept have been developed to improve the power generation efficiency [13,14]. For example, Liu et al. [15] proposed a piezoelectric energy harvesting device based on a frequency up-conversion cantilever stopper to collect energy from low-frequency vibrations. A frequency up-converted piezoelectric energy harvester using mechanical impact is introduced by Halim et al. [16]. Tang and Li [17] presented a frequency up-converted energy harvester with a two-stage vibratory structure. Based on this concept, low-frequency vibration energy can be scavenged by the above designs. Unfortunately, the performance of this type of energy harvester is significantly dependent on the driving element, which is designed for harvesting ambient low-frequency vibrations. The narrow bandwidth of the driving part largely confines the power generation efficiency under the broad range of vibrations in the environment. Furthermore, the physical impact method reduces the reliability and service life of the energy harvester. Additionally, the large frequency gap between a driving part and a power generation part influences to the efficiency in power generation. Aiming for a broad bandwidth to match the environmental vibration, Shahruz [18] presented an energy harvester that consists of 13 piezoelectric cantilevers with various resonant frequencies to provide voltage response over a frequency range of 50–62 Hz. Microelectromechanical system (MEMS)-based piezoelectric cantilever array for vibration energy harvesting that covers a bandwidth of 226–234 Hz was developed by Liu et al. [19]. How-

* Corresponding author.

E-mail address: mems@jnu.ac.kr (D.-W. Lee).

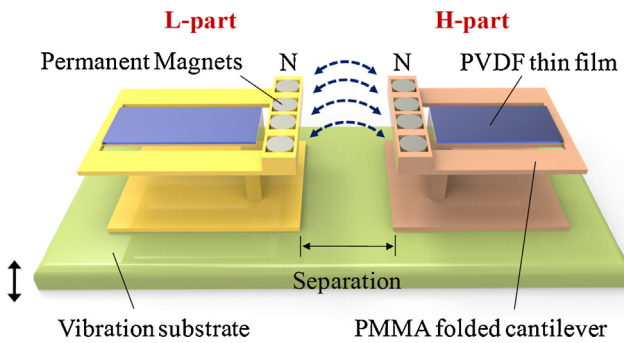


Fig. 1. The designed high-efficiency broadband energy harvester with magnetically coupled folded cantilevers.

ever, for such multi-cantilever (or cantilever array)-based energy harvesters, not only does the narrow response bandwidth of each cantilever restrict the total frequency range of the device, but the numerous cantilevers also decrease space efficiency. Moreover, the frequency-selecting mechanism (only one cantilever can achieve resonance for each excitation frequency) leads to low power generation efficiency when the excitations cover a broad frequency range. Frequency detuning is also one of useful techniques to cover wide ambient frequency range in energy harvester applications. This is realized by adjusting various parameters such as the applied force or the stiffness. Vijayan et al. [20] developed a non-linear energy harvesting method by carefully detuning the frequencies of coupled impacting beams. Neumeyer et al. [21] discussed the possibility of applying the frequency detuning to energy harvesting application.

In this study, a design of an energy harvester based on magnetically coupled folded cantilevers is proposed, which can scavenge environmental vibration energy with high efficiency in a broad frequency range. The proposed energy harvester takes an advantage of the frequency detuning technique and multi-cantilevers to enhance its power generation efficiency for ambient low-frequency excitation.

2. Design and modelling

A schematic of the design is shown in Fig. 1. It can be seen that one piezoelectric energy harvester with a low resonant frequency (L-part) is coupled with the other piezoelectric energy harvester with a high resonant frequency (H-part) through a non-contact magnetic force. To provide the non-contact magnetic force, eight identical permanent NdFeB magnets are mounted on the ends of the cantilevers with the same magnetic pole arrangements. A thin polyvinylidene fluoride (PVDF) film is uniformly attached on the cantilevers to generate power when stress is accumulated on the cantilevers during vibrations. In order to allow both parts to possess their own high-efficiency range in the ordinary range of ambient vibrations in normal conditions, the resonant frequencies of both L-part and H-part are designed within a range of 0–40 Hz (L-part: 18 Hz, H-part: 32 Hz, the detailed process of resonant frequency optimization can be found in Supplementary materials) by adjusting the dimension parameters (i.e., the thickness and length of the cantilever). Moreover, owing to the effect of magnetic coupling, the two parts can enhance each other's output performance even if the ambient excitations deviate from the original resonant zones of the cantilevers. This mechanism is illustrated in detail as the following reasons: (a) When the energy harvester is vibrated in a low-frequency range, the L-part can sufficiently generate power because the ambient excitation matches with its own resonant frequency, meanwhile driving the H-part to produce power with a high efficiency through the non-contact magnetic force. (b) On the

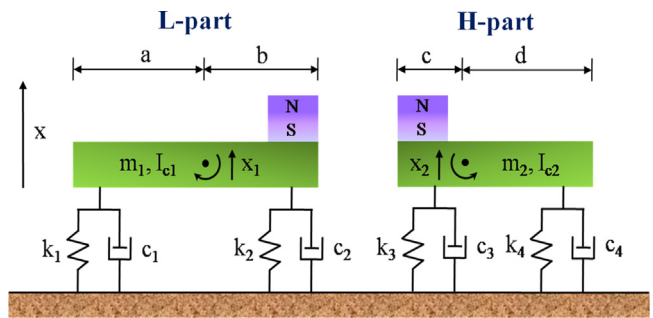


Fig. 2. The dynamic model of the designed energy harvester.

other hand, when the ambient vibration frequency is close to the high-efficiency zone of the H-part (near its natural frequency), the H-part can also promote the deformation/stress of the L-part owing to the non-contact magnetic force; this contributes to the output of the L-part. (c) The variable magnetic forces during the vibration control the resonant frequencies of the two parts in a certain small range due to the frequency detuning mechanism, which allows a broader bandwidth of the energy harvester at ambient conditions. It is noted that the gap between the two resonant frequencies of L-part and H-part will affect the coupling efficiency. If the frequency gap is too large, the coupling efficiency would be weak. On the other hand, the total bandwidth would be narrowed if the two resonant frequencies approaches too close with each other. Aiming for a wide bandwidth and high power generation efficiency, 18 Hz and 32 Hz are utilized as the resonant frequencies for L-part and H-part, respectively. The resonant frequency optimization for the two parts is discussed in the Supplementary materials. Considering that the separation between the L-part and H-part influences the magnetic coupling effect, the separation should be maintained with an optimized distance to achieve maximum output. In addition, folded cantilever structures are designed to further enhance power generation and space efficiency.

In order to investigate the characteristics of the designed energy harvester, a simplified dynamic model is established. As shown in Fig. 2, each part of the designed energy harvester can be modeled as a damped two degree-of-freedom (DOF) mass-spring system. Supported by damped springs with spring constant k_i and damping coefficient c_i ($i = 1\text{--}4$), the equation of motion for the complete model can be expressed as:

$$\begin{bmatrix} m_1 & 0 & 0 & 0 \\ 0 & I_{c1} & 0 & 0 \\ 0 & 0 & m_2 & 0 \\ 0 & 0 & 0 & I_{c2} \end{bmatrix} \begin{bmatrix} \ddot{x}_1 \\ \ddot{\theta}_1 \\ \ddot{x}_2 \\ \ddot{\theta}_2 \end{bmatrix} + \begin{bmatrix} c_1 & 0 & 0 & 0 \\ 0 & c_2 & 0 & 0 \\ 0 & 0 & c_3 & 0 \\ 0 & 0 & 0 & c_4 \end{bmatrix} \begin{bmatrix} \dot{x}_1 \\ \dot{\theta}_1 \\ \dot{x}_2 \\ \dot{\theta}_2 \end{bmatrix} + \begin{bmatrix} k_1 + k_2 & -(k_1 a - k_2 b) & 0 & 0 \\ -(k_1 a - k_2 b) & k_1 a^2 + k_2 b^2 & 0 & 0 \\ 0 & 0 & k_3 + k_4 & -(k_4 d - k_3 c) \\ 0 & 0 & -(k_4 d - k_3 c) & k_4 d^2 + k_3 c^2 \end{bmatrix} \begin{bmatrix} x_1 \\ \theta_1 \\ x_2 \\ \theta_2 \end{bmatrix} = \begin{bmatrix} F_{G1} + F_{mag} \\ -F_{mag}b \\ F_{G2} - F_{mag} \\ F_{mag}c \end{bmatrix} \quad (1)$$

where m_j and I_{cj} ($j = 1$ and 2) are the mass and moment of inertia around the centroid of each cantilever, respectively. F_{Gj} is the

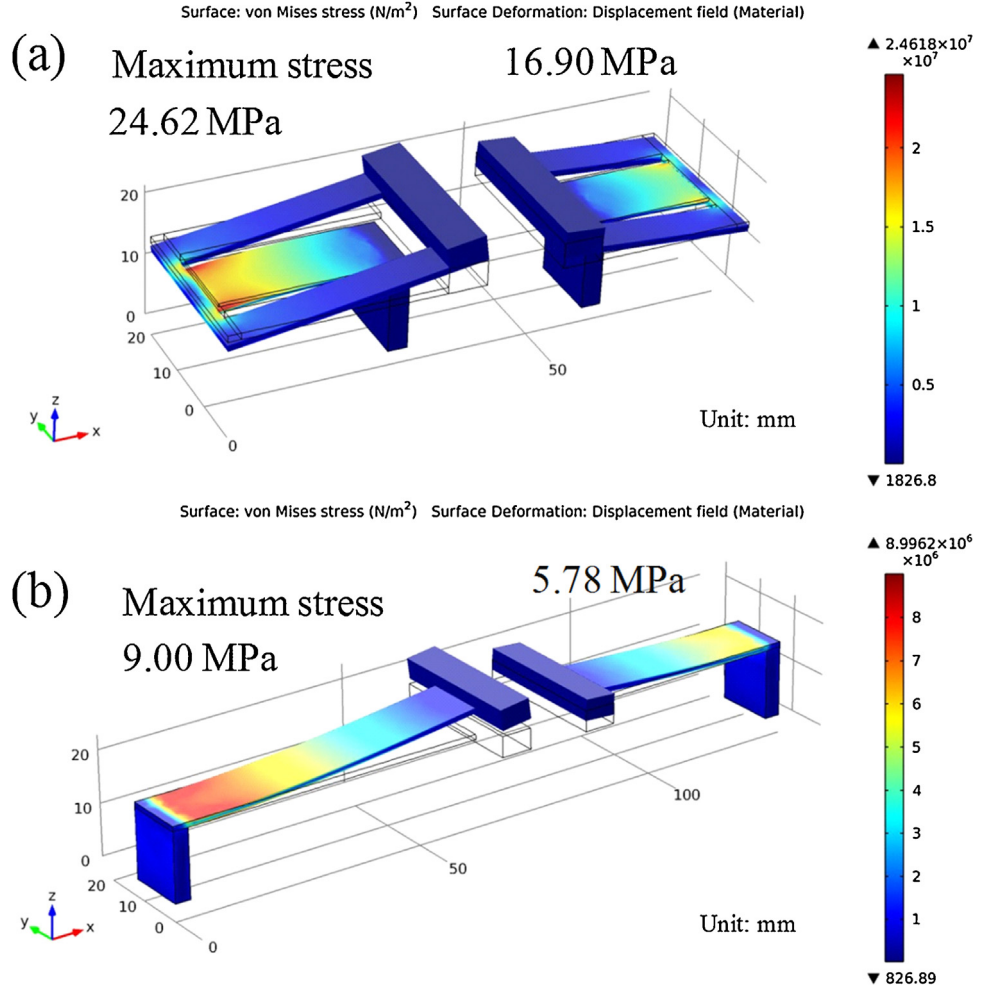


Fig. 3. FEM stress distribution comparison between the (a) folded cantilever and (b) conventional straight cantilever (before folding).

inertial forces acting on the mass m_j . The spring constant k_i can be achieved from following relationship:

$$\begin{cases} |4\pi^2f_1^2 \begin{pmatrix} m_1 & 0 \\ 0 & I_{c1} \end{pmatrix} - \begin{pmatrix} k_1 + k_2 & -(k_1a - k_2b) \\ -(k_1a - k_2b) & k_1a^2 + k_2b^2 \end{pmatrix}| = 0 \\ |4\pi^2f_2^2 \begin{pmatrix} m_2 & 0 \\ 0 & I_{c2} \end{pmatrix} - \begin{pmatrix} k_3 + k_4 & -(k_4d - k_3c) \\ -(k_4d - k_3c) & k_4d^2 + k_3c^2 \end{pmatrix}| = 0 \end{cases} \quad (2)$$

where f_1 and f_2 are the resonant frequencies of L-part and H-part, respectively [22]. Considering that the magnetic force contributes to the coupling effect, the magnetic force between the L-part and H-part in x -direction can be derived. Based on magnetic charge method [23], the interaction energy W between two identical cylindrical magnets can be achieved by:

$$W = \int_{S_1} ds_1 \int_{S_2} ds_2 \frac{\sigma^2}{4\pi\mu_0 r} \quad (3)$$

where S_1 and S_2 are the basal area of the cylinder magnet. σ represents the density of magnetic charges, and μ_0 is the permeability in air. r is the distance between two arbitrary points on the two magnet bases. From the interaction energy, the magnetic force along one direction can be conveniently obtained by:

$$\vec{F} = -g\vec{\text{rad}} W \quad (4)$$

Thus, the magnetic force between two magnets in x -direction is:

$$F_{\text{mag},2} = -\frac{d}{dx} \left(\int_{S_1} ds_1 \int_{S_2} ds_2 \frac{\sigma^2}{4\pi\mu_0 r} \right) \quad (5)$$

Here, 8 identical cylinder magnets are utilized in this design. The magnetic force calculation for more than two magnets was investigated by Vokoun et al. [24]. The magnetic force between the L-part and H-part in x -direction can be derived based on the reference:

$$F_{\text{mag},8} = -\frac{d}{dx} \left(\sum_{i=1}^4 \sum_{j=5}^8 \int_{S_1} ds_1 \int_{S_2} ds_2 \frac{\sigma^2}{4\pi\mu_0 r_{i,j}} \right) \quad (6)$$

where the indices i and j denote the cylindrical magnet bases respectively. $r_{i,j}$ represents the distance between two arbitrary points on the magnet bases. It noted that higher stress and output power could be achieved by using the magnetic force applied to the piezoelectric cantilevers.

To verify the advantages of utilizing the designed folded cantilevers in the energy harvester, finite element method (FEM) simulations are carried out using the COMSOL Multiphysics software. For convenient comparison, models of both the folded cantilever and the conventional straight cantilever are established in the simulation with identical input conditions. Furthermore, the length of the conventional straight cantilever equals to that of the folded cantilever before folding. In the simulation models, the magnets are simplified as a proof-mass but with the same physical properties. The material and parameters of the folded cantilever

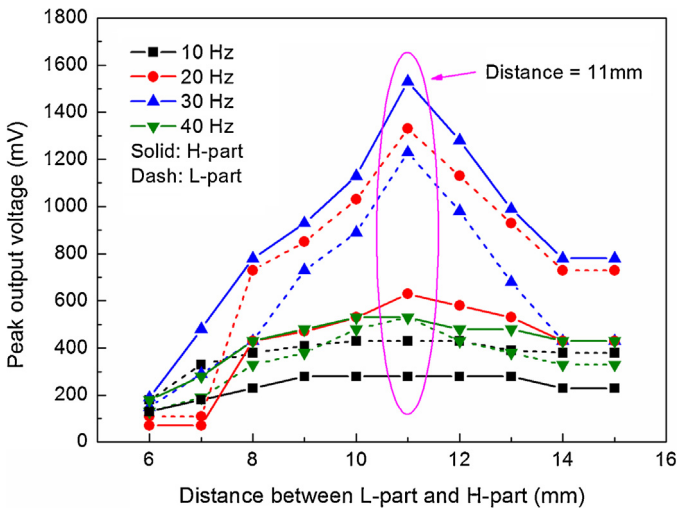


Fig. 4. Optimization of the distance between the L-part and H-part.

models built in this simulation remain the same for the L-part and H-part, respectively. As can be seen from Fig. 3(a) and (b), higher stress can be achieved by using this folded cantilever than by using a straight cantilever. Because a high stress on the piezoelectric material enhances charge accumulation and output, the simulation results prove that the folded cantilever can enhance the power generation capability and vibration energy harvesting efficiency [25–27].

3. Experiment results

In order to evaluate the performance of the design, a prototype of this energy harvester is manufactured using a Projet HD 3500 Plus Professional 3D printer (3D Systems Corp., USA), which can conveniently realize the integrated total structure at low cost [28]. The geometric dimensions and material details of the fabricated energy harvester are listed in Table 1. In the performance test, the energy harvester is mounted on a TIRA Vib BAA 120 shaker (TIRA GmbH, Inc., Germany). Using an Agilent 33120A function generator (Agilent Technologies, Inc., USA), the shaker can produce sinusoidal excitation with various frequencies, thereby vibrating the energy harvester in the vertical direction. The output voltage and power generation frequency is measured using a Tektronix TDS 2014B oscilloscope (Tektronix, Inc., USA).

Considering that the distance between the L-part and H-part affects the magnetic coupling strength, the separation of the two parts is optimized to obtain the most effective coupling effect. When the distance is smaller than 6 mm, the two magnet groups will be attracted together during vibration owing to the strong magnetic force, which results in inefficient working performance under ambient excitations. On the other hand, a distance of more than 15 mm is beyond the coupling ability of the two magnet groups. Therefore, the separation distance is adjusted to be in the range of 6–15 mm for optimization. Fig. 4 shows the relationship between the output and separation distance. It can be seen that when the two parts are magnetically coupled with a small distance, thereby being subjected to the strong constraints of the magnetic repulsive force, the output of the two parts is even lower than that for the condition without coupling. In this condition, the L-part and H-part cannot completely vibrate under excitations. On the contrary, when the distance is increased to 14 mm or larger, the magnetic force is too weak to maintain the coupling mechanism, thereby resulting in an output performance similar to that obtained for the case without coupling. With various gap distances between the two parts, maximum output can be achieved with an 11-mm distance, even

under different vibration frequencies (10, 20, 30, and 40 Hz). Therefore, because the aim is to achieve efficient output capability under the same conditions, the optimized distance of 11 mm is utilized in further experiments.

With the optimized distance, the output performance of the energy harvester is characterized at an acceleration of 0.1 g and a vibration frequency range of 0–40 Hz. As shown in Fig. 5(a), when the excitation frequency is close to the resonant frequency of the L-part (17 Hz), the L-part dominates the power generation with a large cantilever deflection, thereby driving the H-part to vibrate at its own resonant frequency through the non-contact magnetic force. It can be seen that maximum output voltage of 1.5 V and 0.7 V can be achieved by the L-part and the H-part, respectively. When the input vibration frequency reaches the resonant frequency of the H-part (30 Hz), the H-part dominates the output with large deflections owing to the resonance. Because the stiffness of the L-part is lower, the magnetic coupling has greater apparent influence on the L-part, which leads to the L-part having large deformation in this frequency. In this case, compared with the low-efficiency vibration for only the L-part without coupling, the output performance of the L-part can be improved through the non-contact coupling technique. As shown in Fig. 5(b), maximum voltage of 1.5 V and 1.2 V is achieved by the H-part and the L-part, respectively. It should be noted that the original resonant frequencies of the two parts are slightly reduced after coupling with each other, which is attributed to the influence of the magnetic force. Fig. 5(c) shows the output frequency changes of the L-part and H-part under various excitation frequencies in the range of 0–40 Hz. It can be seen that the L-part and the H-part successively dominate the power generation. In this case, the bandwidth and the output performance of the energy harvester are improved by employing the frequency detuning mechanism. On the contrary, when the magnets are replaced by steel masses with equivalent weight to eliminate the influence of magnetic coupling, the frequency detuning mechanism and the increasing output effect is not observed in the experiment.

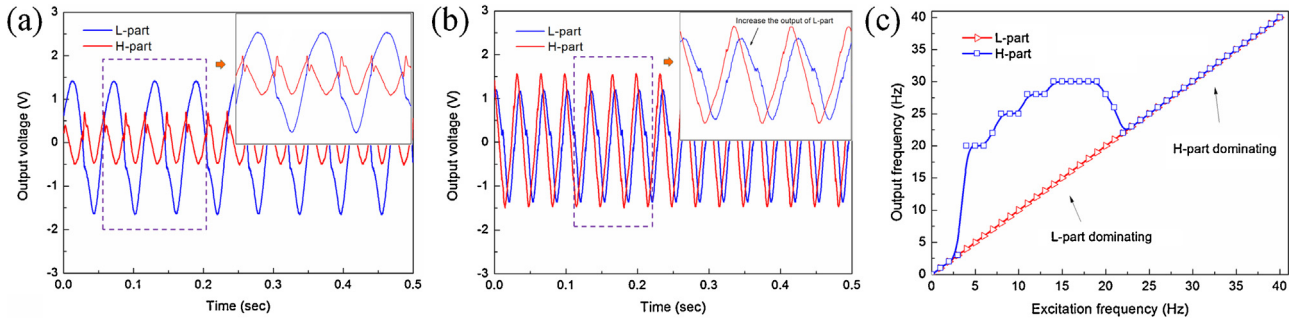
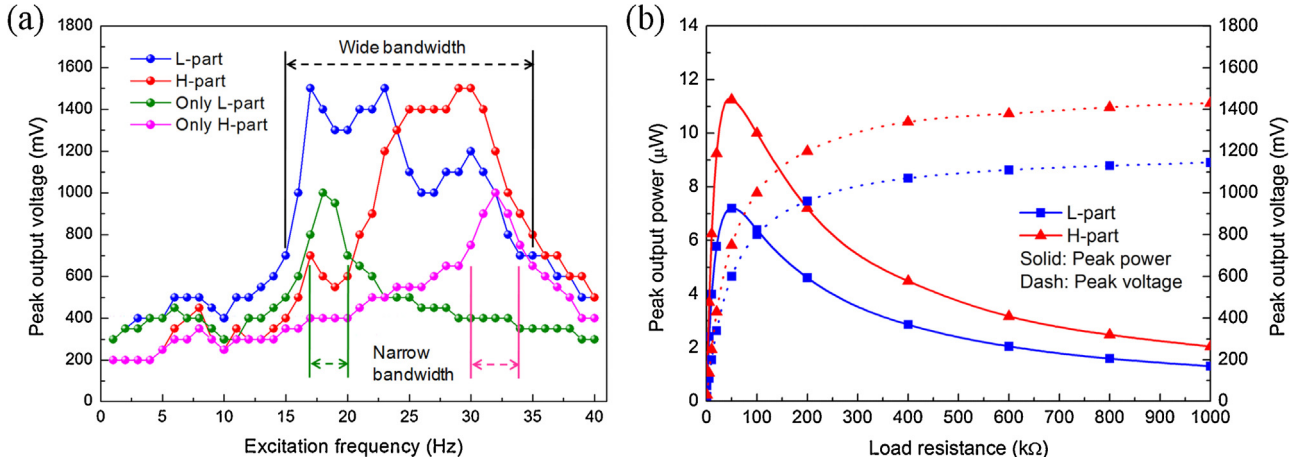
To determine the coupling influence on the bandwidth of the energy harvester, bandwidth characterization before and after magnetic coupling is carried out in a frequency range of 0–40 Hz, as shown in Fig. 6(a). Assuming 700 mV as the high-efficiency threshold, we can see that a broad high-efficiency zone is achieved after non-contact magnetic coupling; this zone is much broader than that before coupling. In addition, it is noted that the peak output voltage of each part is enhanced compared with that before coupling. This is because the magnetic force allows higher stress to be applied to each piezoelectric cantilever, which proves the aforementioned theoretical analysis. Therefore, owing to the non-contact magnetic coupling technique, not only can a significant improvement in the working bandwidth be realized for the energy harvester, but the output performance can also be enhanced. Moreover, a durable lifespan is obtained because of this non-impact driving method. In this manner, the energy harvester proposed in this work can effectively scavenge ambient vibration energy with a broad bandwidth. It should be noted that the lifetime of the energy harvester can also be conveniently improved by replacing PMMA with a stronger material such as steel. The bandwidth of the energy harvester under various acceleration values (0.15 g, 0.1 g, and 0.05 g) has been systematically characterized to study an acceleration force dependency in the coupling effect. The experiment results are listed in the Supplementary materials. These experiment results indicate that the total bandwidth can still be efficiently improved even with a small acceleration force.

According to Jacobi's law, maximum power transmission takes place when the load impedance is equivalent to the output impedance value of the system [29]. In order to transfer the maximum output power, it is necessary to consider the impedance matching of the energy harvester. As shown in Fig. 6(b), different

Table 1

Parameters of the fabricated energy harvester.

Parameters	L-part	H-part
Dimension	39 mm × 28 mm × 15 mm	30 mm × 28 mm × 15 mm
Natural frequency	Before coupling: 18 Hz After coupling: 17 Hz	Before coupling: 32 Hz After coupling: 30 Hz
Material	Polymethylmethacrylate (PMMA)	
End-magnets	Diameter 5 mm, thickness 2.5 mm, NdFeB, 0.14 T	

**Fig. 5.** Output waveform of the energy harvester under an excitation of (a) 17 Hz and (b) 30 Hz; (c) the output frequency of the L-part and H-part versus various excitation frequencies.**Fig. 6.** (a) Bandwidth and output voltage performance of the energy harvester (before and after coupling) and (b) peak output power and load resistance optimization (30 Hz, 0.1 g).

load resistors are connected to the energy harvester with a constant input vibration frequency of 30 Hz. When the load resistance is 50 kΩ, peak output power of 11.25 μW and 7.2 μW are achieved by the H-part and the L-part, respectively (18.45 μW in total).

In order to verify the power generation capability in a practical situation, a feasibility experiment is carried out. In this experiment, the energy harvester is mounted on an air maker, as shown in Fig. 7(a). The energy harvester is excited by vertical vibration during the operation of the air maker (~0.15 g acceleration). It can be seen that maximum output voltages of 0.8 V and 0.6 V are obtained by the H-part and L-part, respectively. With the optimized load resistance (50 kΩ for each), a maximum output power of 20 μW and an average power of 7.1 μW are achieved by the energy harvester. This achieved output power can fully satisfy the minimum power consumption of a sensor node in the WSN applications (<10 μW) [30]. Fig. 7(b) shows a LCD screen lightened by the fabricated energy harvester in such a low-frequency vibration environment. This enables the energy harvester can be employed as a potential power supply for the self-powered electronic devices or an autonomous-powered acceleration meter in the industrial applications.

4. Conclusions

In this study, a high-efficiency piezoelectric energy harvester based on a non-contact magnetic coupling technique was designed and experimentally characterized. The L-part and H-part can improve each other's output performance through this coupling mechanism in an ordinary vibration environment. Folded cantilevers were designed for this energy harvester to enhance space and power efficiency. In performance tests, a broad bandwidth for environmental low-frequency vibration was achieved. Moreover, a LCD screen is lightened by the energy harvester in a vibration ambient provided by an air maker. With an optimized load resistance of 50 kΩ, a peak output power of 20 μW and an average power of 7.1 μW were achieved by the energy harvester in the feasibility experiment, which satisfies the power requirement of WSN applications. In our future work, we will optimize the material for this energy harvester to satisfy more complex working environment, which can be expected to expand its applications.

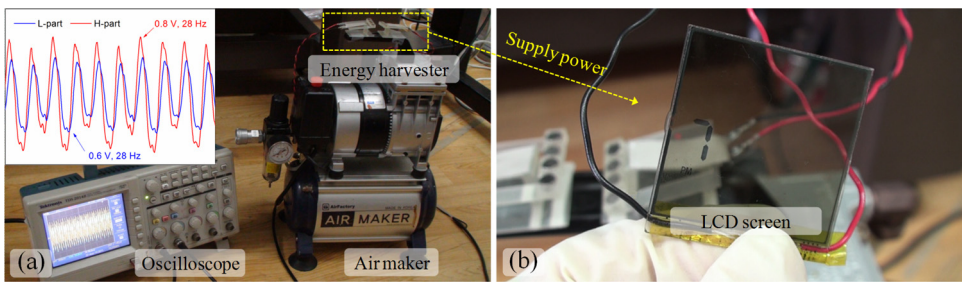


Fig. 7. (a) Performance test for the energy harvester in a vibration environment provided by an air maker and (b) a LCD screen lightened by the energy harvester.

Acknowledgements

This research was supported by National Research Foundation of Korea (NRF) Grant funded by the MEST of the Korean government (No. 2012K1A3A1A20031500 and No. 2015R1A2A2A05001405) and International Collaborative R&D Program through KIAT grant funded by the MOTIE (N00000894).

Appendix A. Supplementary data

Supplementary data associated with this article can be found, in the online version, at <http://dx.doi.org/10.1016/j.sna.2015.08.009>.

References

- [1] I.F. Akyildiz, Wireless sensor networks: a survey, *Comput. Netw.* 38 (2002) 393–422.
- [2] H. Messer, Environmental monitoring by wireless communication networks, *Science* 312 (5774) (2006) 713.
- [3] Q.C. Tang, Y.L. Yang, X.X. Li, Repulsively driven frequency-increased-generators for durable energy harvesting from ultra-low frequency vibration, *Rev. Sci. Instrum.* 85 (45004) (2014) 1–5.
- [4] J. Yang, X.H. Yue, Y.M. Wen, P. Li, Q.M. Yu, X.L. Bai, Design and analysis of a 2D broadband vibration energy harvester for wireless sensors, *Sensor. Actuat. A Phys.* 205 (2014) 47–52.
- [5] X. Wu, D.W. Lee, An electromagnetic energy harvesting device based on high efficiency windmill structure for wireless forest fire monitoring application, *Sensors Actuat. A Phys.* 219 (2014) 73–79.
- [6] G. Cha, Y.S. Ju, Pyroelectric energy harvesting using liquid-based switchable thermal interfaces, *Sensors Actuat. A: Phys.* 189 (2013) 100–107.
- [7] S. Roundy, P.K. Wright, A piezoelectric vibration based generator for wireless electronics, *Smart Mater. Struct.* 13 (5) (2004) 1131–1142.
- [8] A. Bibo, M.F. Daqqaq, Investigation of concurrent energy harvesting from ambient vibrations and wind using a single piezoelectric generator, *Appl. Phys. Lett.* 102 (243904) (2013) 1–4.
- [9] X. Wu, M. Parmar, D.W. Lee, A seesaw-structured energy harvester with superwide bandwidth for TPMS application, *IEEE/ASME Trans. Mechatronics* 19 (5) (2014) 1514–1522.
- [10] W.A. Ashtari, M. Hunstig, T. Hemsel, W. Sextro, Enhanced energy harvesting using multiple piezoelectric elements: theory and experiments, *Sensors Actuat. A: Phys.* 200 (2013) 138–146.
- [11] T. Galchev, H. Kim, K. Najafi, Non-resonant bi-stable frequency increased power scavenger from low-frequency ambient vibration, *Proceedings of Transducers, June 2009* (2009) 632–635.
- [12] J.C. Park, J.Y. Park, Y.P. Lee, Modeling and characterization of piezoelectric d33-mode mems energy harvester, *J. Microelectromech. Syst.* 19 (5) (2010) 1215–1222.
- [13] H. Külah, K. Najaf, Energy scavenging from low-frequency vibrations by using frequency up-conversion for wireless sensor applications, *IEEE Sens. J.* 8 (3) (2008) 261–268.
- [14] S.M. Jung, K.S. Yun, Energy-harvesting device with mechanical frequency-up conversion mechanism for increased power efficiency and wideband operation, *Appl. Phys. Lett.* 96 (111906) (2010) 1–3.
- [15] H.C. Liu, C. Lee, T. Kobayashi, C.J. Tay, C. Quana, Piezoelectric MEMS-based wideband energy harvesting systems using a frequency-up-conversion cantilever stopper, *Sensors Actuat. A: Phys.* 186 (2012) 242–248.
- [16] M.A. Halim, S. Khym, J.Y. Park, Frequency up-converted wide bandwidth piezoelectric energy harvester using mechanical impact, *J. Appl. Phys.* 114 (44902) (2013) 1–5.
- [17] Q.C. Tang, X.X. Li, Two-stage wideband energy harvester driven by multimode coupled vibration, *IEEE/ASME Trans. Mechatronics* 20 (1) (2015) 115–121.
- [18] S.M. Shahruz, Design of mechanical band-pass filters for energy scavenging, *J. Sound Vib.* 292 (2006) 987–998.
- [19] J. Liu, H. Fang, Z. Xu, X. Mao, X. Shen, D. Chen, H. Liao, B. Cai, A MEMS-based piezoelectric power generator array for vibration energy harvesting, *Microelectron. J.* 39 (2008) 802–806.
- [20] K. Vijayan, M.I. Friswell, H.H. Khodaparast, S. Adhikari, Non-linear energy harvesting from coupled impacting beams, *Int. J. Mech. Sci.* 96 (2015) 101–109.
- [21] S. Neumeyer, M.H.M. Van Gastel, V.S. Sorokin, J.J. Thomsen, Frequency detuning effects for parametrically and directly excited elastic structures, *Proceedings of 5th ECCOMAS Thematic Conference on Computational Methods in Structural Dynamics and Earthquake Engineering*, May 2015 (2015) 1–7.
- [22] L. Meirovitch, *Fundamentals of Vibrations, Two-Degree-of-Freedom Systems*, McGraw-Hill, International Edition, New York, 2001, Chapter 5.
- [23] G. Akoun, J.P. Yonnet, 3D analytical calculation of the forces exerted between two cuboidal magnets, *IEEE Trans. Magn.* 20 (5) (1984) 1962–1964.
- [24] D. Vokoun, M. Beleggia, L. Heller, P. Sittner, Magnetostatic interactions and forces between cylindrical permanent magnets, *J. Magn. Magn. Mater.* 321 (22) (2009) 3758–3763.
- [25] J. Sirohi, I. Chopra, Fundamental understanding of piezoelectric strain sensors, *J. Intel. Mat. Syst. Str.* 11 (2000) 246–257.
- [26] Y.M. Zheng, X. Wu, M. Parmar, D.W. Lee, High-efficiency energy harvester using double-clamped piezoelectric beams, *Rev. Sci. Instrum.* 85 (026101) (2014) 1–3.
- [27] X. Wu, D.W. Lee, A high-efficient broadband energy harvester based on non-contact coupling technique for ambient vibrations, *Proceedings of 28th IEEE International Conference on Micro Electro Mechanical Systems (MEMS 2015)* (2015) 1110–1113.
- [28] E. Bassoli, A. Gatto, L. Luliano, M.G. Violante, 3D printing technique applied to rapid casting, *Rapid Prototyping J.* 13 (3) (2007) 148–155.
- [29] J. Liang, W.H. Liao, Impedance modeling and analysis for piezoelectric energy harvesting systems, *IEEE/ASME Trans. Mechatronics* 17 (6) (2012) 1145–1157.
- [30] R. Elfrink, First autonomous wireless sensor node powered by a vacuum-packaged piezoelectric MEMS energy harvester, *IEEE Electron Dev. Meeting* 22 (5) (2009) 1–4.

Biographies



Xuan Wu received the B. Eng. and M. Eng. degrees in mechanical engineering from Chongqing University of Technology, Chongqing, China in 2009 and 2012, respectively. He is currently working toward the Ph.D. degree in mechanical engineering in the MEMS and Nanotechnology Laboratory, Department of Mechanical Engineering, Chonnam National University, Korea. He is the holder of two patents in China. He is also a member of the Korean Sensors Society. His current research interests include energy-harvesting technology, MEMS device design and fabrication, smart materials and structures, liquid metal based devices, and graphene local anodic lithography technology.



Dong-Weon Lee received the Ph.D. degrees in Mechatronics engineering from Tohoku University, Sendai, Japan in 2001. He has been a Professor of Mechanical Systems Engineering at Chonnam National University (CNU), Republic of Korea since March 2004. Previously, he was with the IBM Zurich Research Laboratory in Switzerland, working mainly on micro cantilever devices for chemical AFM applications. At CNU, his research interests include smart cantilever devices, miniaturized energy harvester, smart materials and structures, and nanoscale transducers. He is a member of the technical program committee of IEEE Sensors Conference, Transducers, and Micro processes and Nanotechnology Conference (MNC).